JOURNAL OF GEOPHYSICAL RESEARCH, VOL. 95, NO. D7, PAGES 10,155–10,161, JUNE 20, 1990

An Airborne Compatible Photofragmentation Two-Photon Laser-Induced Fluorescence Instrument for Measuring Background Tropospheric Levels of NO, NO_x, and NO_2

S. T. SANDHOLM, J. D. BRADSHAW, K. S. DORRIS, M. O. RODGERS, AND D. D. DAVIS

School of Earth and Atmospheric Sciences, Georgia Institute of Technology, Atlanta

Reported on is a photofragmentation two-photon laser-induced fluorescence (PF/TP-LIF) sensor with a demonstrated capability for making simultaneous measurements of NO/NO_x/NO_2. This instrumental technique is based on the direct spectroscopic detection of NO via the TP-LIF methodology. The measurement of NO_x (NO + NO_2), and subsequently NO_2, is accomplished by the photofragmentation of NO_2 at 353 nm via a XeF excimer laser. The resultant NO photofragment is then quantitatively detected using the TP-LIF technique. The laser photolysis efficiency for NO_2 is typically 60% for NO_2 photolysis cell residence times of less than 0.5 s. The limit of detection (S/N = 2) for the described PF/TP-LIF instrument is 3.5 pptv for NO (2 min integration time) and 10 pptv for NO_2 (6 min integration time). An assessment of chemical interferences in this system revealed no significant problems. The extension of the PF/TP-LIF methodology to the simultaneous detection of multiple N_xO_y species is discussed.

INTRODUCTION

Because of the pivotal role that reactive odd nitrogen plays in the photochemistry of the natural troposphere [*Crutzen*, 1973, 1979; *Ehhalt and Drummond*, 1982; *Logan et al.*, 1981; *Logan*, 1983; *Singh*, 1987] there has been considerable interest in making reliable measurements of this family of compounds. As a result of this interest, several different types of sensors have been developed to measure background levels of tropospheric NO, NO_x, and NO_2. The recent NASA GTE/CITE 1 program evaluated two types of NO sensors [*Hoell et al.*, 1984; *Beck et al.*, 1987]. The first of these was based on the measurement of chemiluminescence resulting from the reaction $NO + O_3 \rightarrow NO_2^* + O_2$ [*Torres*, 1985; *Carroll et al.*, 1985; *Ridley and Howlett*, 1985]. The second instrumental method involved the direct spectroscopic detection of NO using the two-photon laser-induced fluorescence (TP-LIF) methodology [*Bradshaw et al.*, 1985]. Based on the success of these NO instrument intercomparison tests, a new initiative was implemented, GTE/CITE 2, that involved testing and evaluating several new NO_x/NO_2 sensors [*Hoell et al.*, 1984; *McNeal et al.*, 1983; *Beck et al.*, 1987]. Three of these sensors used independent measurements of NO_x and NO to derive values for NO_2 (i.e., NO_x − NO = NO_2), whereas the fourth method was capable of direct spectroscopic detection of NO_2. The approach taken in the first three measurement systems involved the conversion of NO_2 to NO followed by independent measurements of (converted plus ambient) NO plus (ambient) NO. The three methods of conversion and detection consisted of (1) the use of a spectrally broadband continuous wave (CW) arc lamp to photolyze NO_2 with simultaneous dual-channel detection of NO_x and ambient NO via NO/O_3 chemiluminescence [*Ridley et al.*, 1988], (2) a ferrous sulfate NO_2 converter with sequential single-channel measurement of NO_x and ambient NO via NO/O_3 chemiluminescence [*Ridley et al.*, 1988], and (3) a narrow-band excimer-laser photolytic NO_2 converter with simultaneous dual-channel detection of NO_x and ambient NO via TP-LIF as reported in this paper. As noted above, the fourth NO_2 detection system involved the direct spectroscopic detection of NO_2. In the latter system a tunable diode laser was employed in conjunction with IR absorption spectroscopy [*Hastie et al.*, 1983; *Schiff et al.*, this issue].

During the time period of August 15 through September 6, 1986, the NASA GTE/CITE 2 program conducted 11 aircraft intercomparison flights aboard an L-188C Electra. One of the major goals of this program was to test and evaluate NO_2/NO_x sensor performance under airborne field deployment conditions via instrument intercomparison. The results of this double-blind instrument intercomparison have been presented by the NASA program office [*Gregory et al.*, this issue]. Reported here are the instrumental configuration and operational characteristics of the NO_x/NO_2 sensor labeled GIT-PF/LIF [*Gregory et al.*, this issue].

GENERAL DESCRIPTION OF PF/TP-LIF METHODOLOGY

Details on the first-generation aircraft compatible TP-LIF NO technique, deployed during the fall 1983 NASA GTE/CITE 1 program, have been previously reported on [*Bradshaw et al.*, 1985; *Hoell et al.*, 1984, 1987]. The TP-LIF NO detection system defines the central core of the new NO_x/NO/NO_2 PF/TP-LIF sensor. Very briefly, the TP-LIF NO detection methodology is based upon the spectroscopically selective stepwise laser excitation of specific rovibronic (rotational-vibrational) transitions in the $X^2\Pi \rightarrow A^2\Sigma^+$ system near 226 nm and the $A^2\Sigma^+ \rightarrow D^2\Sigma^+$ system near 1.1 μ. The resultant fluorescence from this excitation process takes place from $D^2\Sigma^+ \rightarrow X^2\Pi$ transitions and thus can be monitored near 187 nm as shown in Figure 1.

To extend the capability of the TP-LIF NO detector to the detection of NO_x/NO_2, and NO_2 photolytic converter was added to the TP-LIF system. This converter is based on the photofragmentation of NO_2 at a spectrally narrow wavelength at 353 nm, e.g.,

Paper number 89JD02779.
0148-0227/90/89JD-02779$05.00

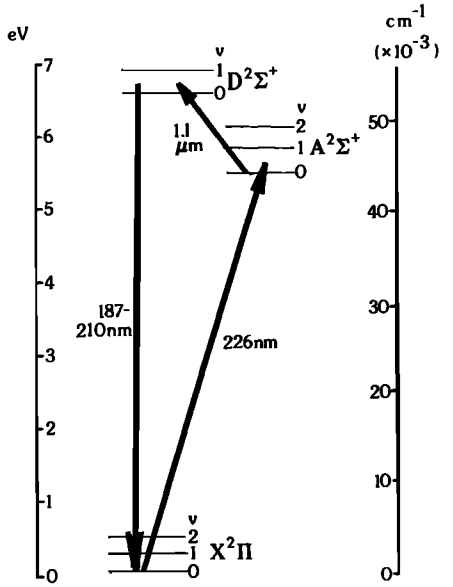

Fig. 1. Energy level diagram showing transitions employed in the two-photon laser-induced fluorescence (TP-LIF) detection of NO.

$$NO_2 + h\nu_p \xrightarrow{\lambda_p = 353\ nm} NO\ (X^2\Pi,\ v'' = 0, 1, 2) + O^3P \quad (1)$$

$$NO\ (X^2\Pi,\ v'' = 0, 1, 2) + M \xrightarrow{k\nu_2} NO\ (X^2\Pi,\ v'' = 0) \quad (2)$$

$$O^3P + O_2 + M \xrightarrow{k_3} O_3 \quad (3)$$

For conditions relevant to the troposphere one finds that both rotational and vibrational relaxation within the $X^2\Pi$ manifold occurs in times of ≤ 4 μs, thereby allowing for complete room temperature thermalization of the NO($X^2\Pi$) state prior to excitation at 226 nm. In addition, for any nominal tropospheric level of NO_2 (e.g., ≤ 100 ppbv) the rapid reaction of $O^3P + O_2 \rightarrow O_3$ ([M] $[O_2] > 10^4\ s^{-1}$) eliminates any possible complication due to secondary chemistry involving the O^3P species. Finally, because of the short transit time through the sampling manifold, chemical complications arising from O_3 are insignificant.

While appearing very similar to the CW arc lamp NO_2 photoconverter developed by *Kley and McFarland* [1980], the laser-based photoconverter described here offers several unique advantages. The high degree of collimation inherent in a laser source (i.e., approximately thirtyfold decrease in beam divergence relative to an arc lamp) allows for the more effective use of long path length photolysis cells. The latter feature makes possible the optimization of the photolysis rate and sample residence time without compromising the integrity of the photolysis convertor with problems such as wall photolysis effects. A second advantage involves the limitation of the photolysis wavelength to $\lambda > 350$ nm. As a result the laser-based system has minimal photolytic interferences arising from the concomitant photolysis of gas-phase species such as alkyl nitrates. Still a final advantage of a laser photoconverter is the practicality of using short sample residence times (i.e., ≤ 1 s) when operating near ambient temperatures and pressures. The latter sampling conditions reduce the possibility of interferences arising from the thermal decomposition of species such as HO_2NO_2 and N_2O_5. The one obvious disadvantage of the laser photoconverter is its complexity and hence its higher susceptibility to failure.

Detailed Description of Experimental Hardware and Technique

Second-Generation TP-LIF NO System

Several significant hardware changes were incorporated into the TP-LIF NO instrument used during the CITE 2 program. This activity was focused in two areas: (1) reduction in the number of driver lasers required to generate the 226-nm and 1.1-μ NO excitation wavelengths and (2) incorporation into the system of multiple fluorescence detection packages to accommodate the simultaneous detection of NO_x and NO. Neither of these hardware alterations adversely affected the overall performance of the TP-LIF technique as previously described by *Bradshaw et al.* [1985].

The basic laser/detection system is shown in Figure 2. It can be seen that unlike the system described by Bradshaw et al., which utilized tandem Nd:YAG pumped dye lasers to separately produce the two excitation wavelengths at 226 nm and 1.1 μ, the new TP-LIF system used only a single high-energy Nd:YAG pumped dye laser (e.g., Quanta Ray DCR 1). The latter change was made possible due to the purely coincidental spectral overlap of the pressure-broadened NO transitions near 226 nm ($X^2\Pi \rightarrow A^2\Sigma^+$) and 1.1 μ ($A^2\Sigma^+ \rightarrow D^2\Sigma^+$) with laser wavelengths that could be generated by the fundamental dye laser wavelength centered near 574 nm.

The second major change to the first-generation airborne TP-LIF NO system involved the use of stacked sampling cell/optical detection packages. The latter change allowed for the use of two or more NO detection cells that simultaneously shared both the 226-nm/1.1-μ laser excitation beams.

The current PF/TP-LIF system has an aircraft footprint of 1.1 m × 2.1 m, an overall weight of 900 kg, and a power utilization of 6.5 kW. This represents a reduction of nearly a factor of 2 in all three categories as compared to the first-generation airborne TP-LIF NO sensor.

Ambient Sampling Manifold

The ambient sampling manifold consisted of separate sampling lines for both NO and NO_x. These lines consisted of PFA Teflon tubing, 1.9 cm OD × 1.6 cm ID, that were thermally insulated. The aircraft inlets were mounted on a zenith observation port, approximately 15 m from the aircraft nose. That portion of the flow line which was external to the aircraft consisted of Teflon tubing encased in a stainless steel tube that extended approximately 0.4 m from the aircraft skin. The latter protective metal tube was bent 90° and pointed the inlet opening aft. Calibration gas was added at a point near the zenith mounting plate. The total distance from inlet to sample cell (or photolysis cell) was approximately 4 m. The residence times in these flow lines were approximately 1 s and 0.6 s for the nominally used volumetric flow rates of 60 Lpm (NO_2) and 100 Lpm (NO), respectively.

Photolytic Converter

The XeF excimer laser used in this system was a Spectra Physics EXC-1 as modified by our group at Spectra-

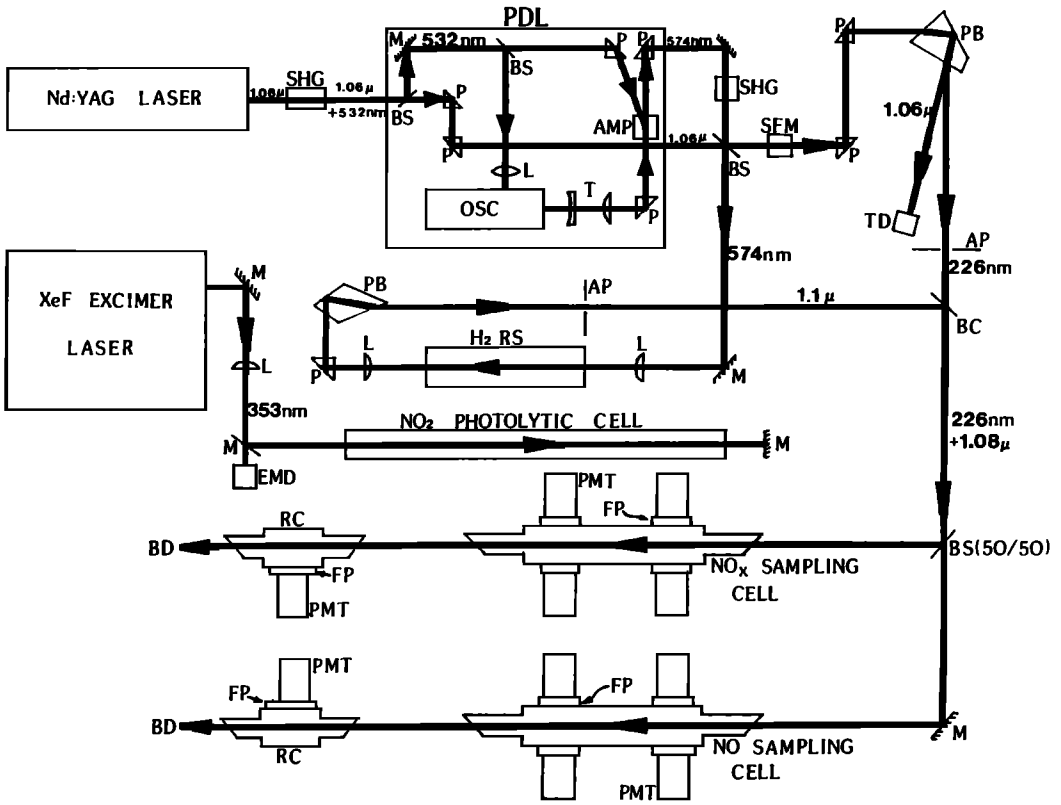

Fig. 2. Schematic representation of PF/TP-LIF instrument (simplified two-dimensional representation without three-dimensional beam steering towers): AMP, dye laser amplifier; AP, aperture; BC, beam-combining mirror; BS, beam-splitting mirror; EMD, energy monitor diode; FP, collection optics/filter pack; (H_2RS, hydrogen Raman shifter; L, focusing lens; M, dichroic mirror; P, 90° prism; PB, Pellin-Brocca prism; PMT, photomultiplier tube; PDL, pulsed dye laser; RC, reference cell; T, beam expansion telescope; and TD, trigger diode.

Technologies. This laser was capable of producing in excess of 14 W of optical power at a wavelength of 353 nm in a 1 cm × 1 cm beam area. Under field sampling conditions the average optical power delivered to the cell was limited to approximately 5 W both due to problems encountered in operating the system at high pulse repetition rates at high altitude and due to losses in the optics train preceding the photolysis cell. The fluency of this system (~5 W/cm^2) can be compared to that from a Cermax 300-W illuminator, e.g., ~0.7 W/cm^2, used in most arc lamp photolytic converter designs (based on an average power/unit area over a 70-nm NO_2 actinic region).

The photolysis cell design used in our system (see Figure 3) consisted of a vacuum-jacketed 2.2-cm-ID × 1-m-long pyrex cell with 1.5-cm-ID gas flow inlet/exhaust ports at each end. This cell design allowed the excimer beam to traverse the 2-m round trip cell distance (double-pass configuration) with minimal energy reaching the sampling cell wall. A 1.5-m focal length lens was used to compensate for laser beam divergence within the photolysis cell region, producing a 0.7 cm × 0.7 cm beam waste near the double pass back reflector.

Using the formalism previously employed by our group [*Rodgers et al.*, 1980, 1985; *Bradshaw and Davis*, 1982; *Bradshaw et al.*, 1985], the single-pulse photolysis efficiency, E_{sp}, can be defined in terms of

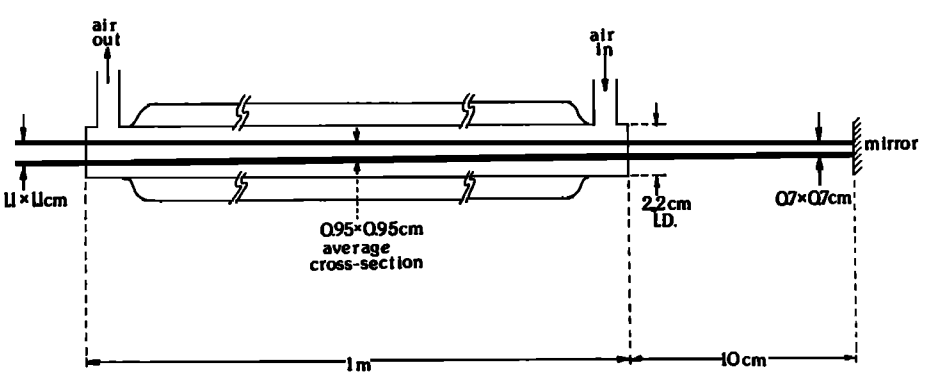

Fig. 3. Details of NO_2 photolysis system showing relevant dimensions of photolysis cell and excimer laser beam.

$$E_{sp} = \phi[1 - \exp(-P_p\sigma_p/a)] \quad (4)$$

where ϕ is the photolytic quantum yield for production of NO at photolysis wavelength λ_p, σ_p is the absorption cross section for NO_2 at wavelength λ_p, P_p/a is the per pulse photon flux at λ_p in units of photons/cm^2. At the wavelength λ_p = 353 nm it is readily shown that $E_{sp} < 0.1$ for the laser energies used in the field system. Thus for a single pulse, nonlinear optical behavior should not be exhibited, and equation (4) can be simplified to the form

$$E_{sp} = \phi(P_p\sigma_p/a) \quad (5)$$

The linear flow velocity within the photolytic sampling cell was in the range of 40 cm/s to 400 cm/s over the range of ambient flow rates used (i.e., 10–100 slpm). This linear flow velocity range provided sample turnover times, Δt_r, of 2.5 s to 0.25 s, respectively. Thus at a nominal laser repetition rate of 180 pulses per second (pps), 450 to 45 individual pulses could interact with the sampled air stream within the cell residence time indicated. The expression therefore which defines the degree of photoconversion of NO_2 to NO during its residence time in the photolysis cell is given by

$$E_p = \left[1 - \exp\left(-\frac{P_t\Delta t_r\sigma_p\phi}{a_{eff}}\right)\right] \quad (6)$$

where P_t is the total laser fluency within the photolysis cell in units of photons per second for the double-passed laser beam, Δt_r is the sample residence time within the photolysis cell (volume of cell/volumetric flow rate), σ_p is absorption cross section for NO_2 ($\sigma_p = 4.9 \times 10^{-19}[1 - 0.0023(298 - T)]$), ϕ is the photolytic quantum yield (0.94) for production of NO (included now in the exponential term, since the return of excited, nondissociated NO_2 to the ground state occurs on a time scale that is rapid compared to the time between pulses, i.e., <1 ms), and a_{eff} is the effective photolysis area for the laser beam interacting with the NO_2 sample during the residence time Δt_r. The latter term, a_{eff}, can be evaluated with the following assumptions: (1) for a pipe flow Reynolds number in the range of 750–7500, applicable to our system, only for the lowest flows would laminar flow conditions prevail, and (2) the half-folding time due to diffusion of NO_2 in and out of the laser photolysis volume is of the order of 100–250 ms, thus allowing this term to dominate the cell mixing at low Reynolds numbers. Under these conditions, with half-folding times for diffusive and turbulent mixing components of less than 200 ms, the total gas volume of the photolysis cell would effectively interact with the volume encompassed by the photolysis laser beam. With these assumptions we have taken the value for a_{eff} = 2.8 cm^2 based on an effective sample cell diameter of 1.9 cm (15% decreased in total ID to account for boundary layer effects on mixing near the cell wall). Thus the final working equation for defining the photolysis efficiency of this system can be expressed as

$$E_p = \left[1 - \exp\left(-C\,\frac{\text{laser power}}{\text{volumetric flow rate}}\right)\right] \quad (7)$$

where (1) the laser power is in watts (measured at the entrance to the photolysis cell), (2) the volumetric flow rate is expressed in liters per minute, and (3) C is a constant which includes the terms V_c (volume of cell) σ_p, ϕ, a_{eff}, and the necessary unit conversion terms. The value of C for this system is calculated to be 11 ± 3, the specified uncertainty mainly reflecting the uncertainty in the value of a_{eff}.

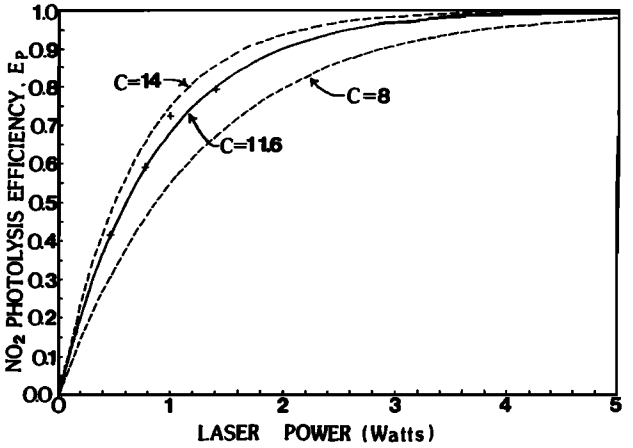

Fig. 4. NO_2 photolysis efficiency, E_p, versus laser power (watts) at a volumetric flow rate (VFR) of 9.6 Lpm. Also shown are theoretical curves for C = 11.6 and the bounds presented by the a priori calculation of C (i.e., C = 11 ± 3).

Figure 4 shows a plot of E_p versus laser power for a fixed flow rate. The best fit of equation (7) to the experimental points gives an empirical value for C of 11.6 ± 0.07. Figure 5 shows a plot of the value of C as a function of volumetric flow rate. As can be seen, all the data points lie within 2σ of the mean, yielding C = 11.6 ± 0.3. In both Figures 4 and 5, E_p was evaluated from the measured NO signal strength for a known concentration of NO_2.

During the CITE 2 program the XeF excimer photolytic converter was nominally operated at 4.5 W. At a typical flow rate of 60 slpm, this resulted in nominal conversion efficiencies for NO_2 of 60%. The total conversion efficiency range covered during CITE 2 was 35–90%. Sample residence times were approximately 0.65 s and 0.35 s for the sample manifold and photolysis cell, respectively.

Calibration System

The calibration system was essentially the same as that described previously [*Bradshaw et al.*, 1985]. However, for the PF/TP-LIF system, a second near-identical three-stage serial dilution system was added to make possible reliable independent NO and NO_2 calibrations. The primary standard for NO_2 consisted of an NO_2/N_2 mixture in an aluminum cylinder. At the several tens of ppmv level these mixtures have exhibited stability for time periods in excess of 5 years as determined by near-UV absorption at the wavelengths 405 nm, 365 nm, and 312 nm using the published absorption cross section for NO_2 published by *DeMore et al.* [1987]. Based on UV absorption measurements, we determined the NO_2 concentration level of our field-deployed primary standard to be 44 ± 3 ppmv, in good agreement with the certified value provided by the vendor of 46 ± 3 ppmv. The working standards employed during our CITE 2 consisted of nominally 50-ppmv NO_2 in air, again housed in aluminum cylinders. Air was chosen as a diluent gas for these high-pressure gas standards to reduce the concomitant NO level. For example, we have found that the NO level can

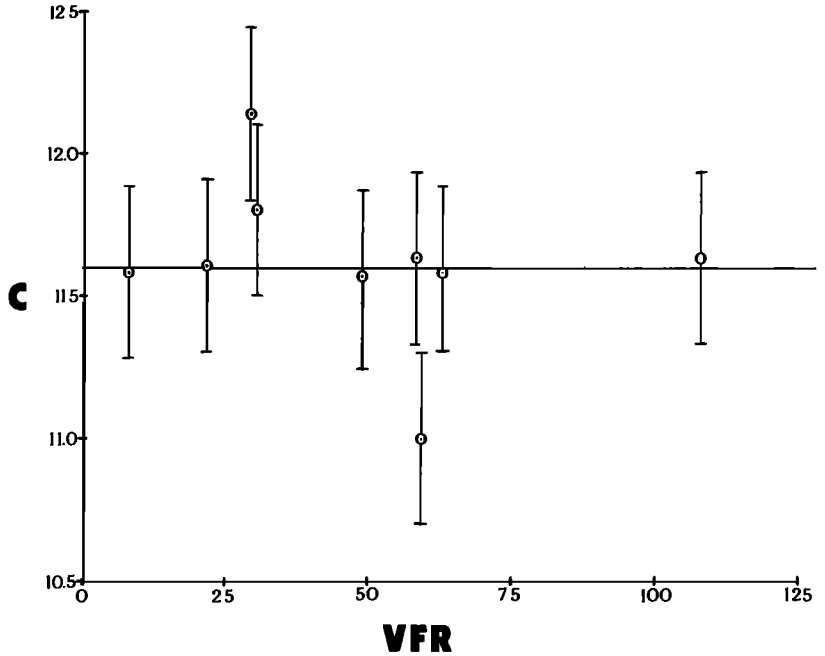

Fig. 5. NO_2 photolysis efficiency exponential constant, C, versus volumetric flow rate (VFR) in liters per minute for a fixed excimer laser power (~4 W). Uncertainties represent 1σ confidence limits.

approach 20% of the nominal NO_2 value in the case where N_2 is used as the diluent gas. In general, however, the long-term stability of NO_2/air mixtures was found to be significantly worse than that for NO_2/N_2 mixtures. Another operational constraint imposed by the use of NO_2/air standards involves the minimum flow rate from the cylinder/gas regulator system. We have found that below approximately 500 standard cubic centimeters (sccm), significant problems can be experienced in obtaining reproducible results, e.g., approximate twofold decrease in observed [NO_2] at 10 sccm versus 500 sccm.

To circumvent the above problem, we have used a bypass flow loop in connecting up to the first stage of our calibration system, thus permitting higher gas cylinder/regulator flow rates. As noted in the accompanying intercomparison paper [*Gregory et al.*, this issue], failure to activate this bypass flow loop system resulted in procedural calibration problems in the early phase of the CITE 2 intercomparison program.

Derivation of [NO_2] From Simultaneous NO_x and NO Measurements

As described earlier in the text, two sampling/detection cells were utilized in our system, one for measuring ambient NO and the second for measuring ambient NO_x.

The equation used to derive ambient NO_2 concentrations from NO_x measurements is given by

$$[NO_2] = \frac{S_{NO_x} - (S_{NO}CR)}{CF_{NO_2}} \quad (8)$$

where S_{NO_x} and S_{NO} represent the net signal counts for the NO_x and NO sample cells, CF_{NO_2} represents the NO_2 calibration factor as determined by periodic NO_2 standard addition spikes to ambient air (normalized to any changes in the photolysis efficiency, E_p), and CR is the measured ratio of detection sensitivities for NO in both the NO and NO_x sampling cells.

In addition to the normalization for changes in the photolysis efficiency, several other small corrections were made to the raw signal count in arriving at a final value for the ambient level of NO_2. The first of these involved a photon counter pileup correction. For NO_x concentrations less than 100 pptv, this was typically less than 10%. The raw signal count rate was also normalized for changes in the TP-LIF system performance (e.g., drift in 226-nm or 1.1-μ laser energy or wavelength). This was accomplished via comparison of signal strengths from a continuously monitored reference cell containing a known concentration of NO, as previously described by *Bradshaw et al.* [1985]. The latter normalization was nominally less than 15%. A final correction to the raw signal involved the laser-induced background noise associated with the 226-nm UV excitation wavelength. This noise was periodically checked by blocking the 1.1-μ IR probe laser and/or by spectrally tuning the probe lasers off resonance with an NO transition. The magnitude of this noise component was typically less than 1 photon/min and therefore usually neglible.

Precision and Accuracy

As described in our previous paper, the TP-LIF NO detection methodology is basically signal limited for integration times of ≤5 min. The precision of these measurements essentially follows that predicted by simple photon statistics of the observed number of total counts, N, for a given integration period (i.e., $\sigma = \sqrt{N}$). The situation is somewhat more complicated for extraction of NO_2 mixing ratios from the measurement of NO_x as given in (8). In this case the statistical uncertainty in the independent NO measurement can greatly influence the overall uncertainty associated with extracting NO_2 concentration levels from NO_x measure-

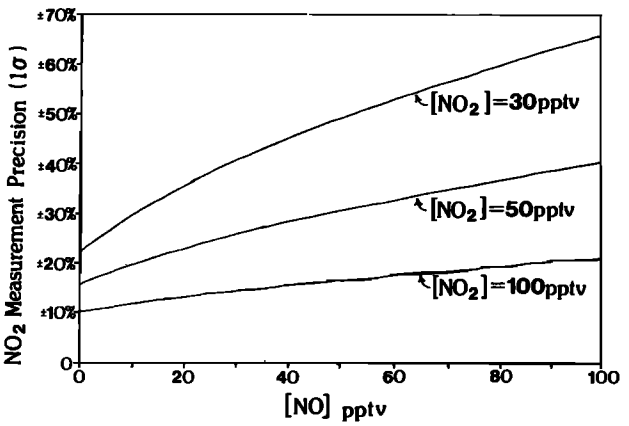

Fig. 6. NO_2 measurement precision versus NO mixing ratio (pptv) where precision is expressed at the 65% confidence level (i.e., 1σ).

ments. Figure 6 illustrates this for a set of nominal conditions experienced during the CITE 2 mission, involving several different ratios of $[NO_2]/[NO]$. The 2σ "total" uncertainty (i.e., combined precision and accuracy estimates) quoted in the GTE/CITE 2 intercomparison paper [*Gregory et al.*, this issue] was given only for the specified ratio $[NO_2]/[NO]$ = 3.3 at NO_2 concentration levels of 30, 50, and 100 pptv. The 2σ "total" uncertainties quoted for these NO_2 levels were ±20, ±23, and ±31 pptv, respectively, for 6-min integration times. These "total" uncertainty estimates were derived by quadratically combining σ_{NO_2} (where $\sigma_{NO_2} = [\sigma_{NO_x}^2 + (CR \times \sigma_{NO})^2]^{1/2}$) and σ_{cal}, then linearly adding the estimated accuracy for the primary to working standard calibration transfer.

The limit of detection (LOD) (S/N = 2/1) for the PF/TP-LIF instrument deployed in the 1985 CITE 2 program was 3.5 pptv for NO, based on a 2-min integration. At concentrations 10 times greater than the LOD, the 1σ precision was ±4.5 pptv. The limit of detection (S/N = 2/1) for NO_2 was on average 10 pptv for a 6-min integration period. At concentration levels fivefold greater than the LOD, the 1σ precision was ±6.5 pptv. Both the LOD and measurement precision were found to vary by approximately a factor of ±1.5 during the CITE 2 operation.

Evaluation of Potential Interferences

Potential photolytic and chemical interferences for the TP-LIF NO technique appear to be ≤2 pptv [*Bradshaw et al.*, 1985]. In this text therefore we will only address the potential interferences in the NO_x/NO_2 measurements.

The production of either NO or NO_2 from any N_xO_y species via direct photolysis at 353 nm would result in an apparent artifact signal in a PF/TP-LIF NO_x (NO + NO_2) measurement. The signal strength from these species would again be given by equations (7) and (8). The absorption cross section for a variety of potentially interfering gases can be found in reviews by *Okabe* [1978], *Demore et al.* [1987], and *Finlayson-Pitts and Pitts* [1986]. For the species N_2O, HNO_3, and HO_2NO_2 (having $\sigma_p < 1 \times 10^{-22}$ cm^2) the calculated photolytic interferences would be <1 pptv for mixing ratios of 200 ppbv, 1 ppbv, and 1 ppbv, respectively. For the species PAN, PPN, and N_2O_5 (having $10^{-22} \leq \sigma_p \leq 2 \times 10^{-21}$ cm^2), given the worst case conditions of $[PAN]/[NO_x]$ = 20 and $[N_2O_5]/[NO_x]$ = 5 and quantum yields of unity for the production of either NO or NO_2, the maximum equivalent NO_2 interference calculated would be less than 2 pptv for mixing ratios of 500, 50, and 200 pptv, respectively [see *Fahey et al.*, 1986]. For the species ClNO, $ClONO_2$, ClONO, $ClNO_2$, HONO, N_2O_3, N_2O_4, CH_3ONO, and $(CH_3)_3CONO$, all of which possess significant absorption cross sections at 353 nm (i.e., $\sigma_p > 10^{-19}$ cm^2/molecule), one would estimate significant interference if these species were present at significant concentration levels in the troposphere. However, because of the absence of effective formation pathways coupled with efficient destruction mechanisms these species are not expected to reach mixing ratios of >5% $[NO_2]$. Under these conditions they should contribute interference signals of ≤5% $[NO_2]$. The last group of compounds CH_3NO_2, $C_2H_5NO_2$, CH_3ONO_2 and $C_2H_5ONO_2$ represent what may be considered rather long-lived species owing to small absorption cross section at wavelengths greater than 300 nm (i.e., $1 \times 10^{-20} > \sigma_p > 2 \times 10^{-21}$ cm^2). Taking $[R'NO_x] = 0.5 \times [PAN] = 20 \times [NO_2]$ as a worst-case situation, we would expect the maximum interference from this class of compounds to be <20% $[NO_2]$. However, it should be noted that for the latter class of compounds, care must be exercised in choosing both the operational value of $E_p(NO_2)$ and the lower bound photolysis wavelength, a potentially serious problem in the case of arc lamp photoconverters.

Another potential interference in the use of the PF/TIP-LIF technique, as well as all other techniques for measuring NO_2, involves the thermal decomposition of pernitric acid, HO_2NO_2, and N_2O_5.

$$HO_2NO_2 \rightleftarrows HO_2 + NO_2 \quad (9)$$

$$N_2O_5 \rightleftarrows NO_2 + NO_3 \quad (10)$$

The equilibrium constants for the above processes show a strong temperature dependency in the region of 250–300 K, changing by approximately 10^3 fold over this temperature range. Under worst-case conditions (i.e., ambient air warming to aircraft cabin temperatures prior to photolytic conversion) the forward rate for reactions (9) and (10) yields decay times at 300 K of 10 and 17 s, respectively. Based on our volumetric flow rates used during CITE 2, the residence time in the sampling line/photolysis cell was <1.5 s. As an additional precaution the sampling line and photolysis cell were thermally insulated, yielding T (sample gas) − T (ambient) of <10 K with a thermal time constant of ~5 min. Therefore the gas-phase homogenous thermal decomposition of HO_2NO_2 and N_2O_5 should have contributed at most a 5% effect for $[HO_2NO_2]/[NO_2]$ and $[N_2O_5]/[NO_2]$ ratios of 2/1. More insidious, however, is any estimation of the surface-catalyzed heterogeneous decomposition of these species on the flow line walls. Our flow line was designed to minimize surface to volume ratios while maintaining short residence times. Attempts at quantifying the potential levels of the former interference during the CITE 2 operation proved inconclusive [*Gregory et al.*, this issue]. As of this writing the magnitude of the potential surface-catalyzed decomposition of either HO_2NO_2 and N_2O_5 also has not been quantified.

A final potential interference involves the reverse titration of the NO photolytic product by ambient O_3, both inside the photolytic convertor and in the sampling volume between

the photolytic convertor and the point of TP-LIF probing (approximately 500 cm^3). This gas-phase titration involving process (11),

$$NO + O_3 \rightarrow NO_2 + O_2 \quad (11)$$

(where $k_{11} = 1.0 \times 10^{-15}$ cm^3 molecule/s at $T = 263$ K), is capable of back titrating the photolytically produced NO prior to TP-LIF probing. Under worst-case tropospheric conditions (i.e., 300 ppbv O_3 at 500 mbar of pressure) the maximum effect of this NO titration reaction would be <6% for the lowest volumetric flow rate used during the CITE 2 mission (i.e., 30 sLpm).

Conclusions

We have demonstrated the utility of a PF/TP-LIF sensor for the detection of $NO/NO_x/NO_2$. An extensive examination of both photolytic and thermally induced interferences involving other N_xO_y compounds at nominal atmospheric levels suggests that no significant interferences should influence PF/TP-LIF measurements of $NO/NO_x/NO_2$. Simultaneous measurements of other N_xO_y species now seems possible with minimal alteration of this instrument.

Looking to the future, we see the major effort on this technique being further improvements in sensitivity. The goal in this case would be to reach detection limits of ~1 pptv for NO and NO_x with integration times of <1 min. This increase in sensitivity will be necessary to meet several of the future needs of the field of atmospheric chemistry.

Acknowledgments. The authors would like to acknowledge the support of this research by NASA grant NAG-1-50 and the Coordinating Research Council (CRC project CAPA-23/24). They would also like to express their appreciation to Roger Navarro for the support received from the NASA Wallops Flight Facility for the flight operations on the NASA L-188 Electra via the GTE/CITE 2 program office. They express their special thanks to Jim Hoell, Gerry Gregory, and Richard Bendura for their patience and guidance throughout the GTE/CITE 2 NASA program. Finally, they would like to compliment the NASA GTE program office on their dedication to providing instrument validation programs of high integrity.

References

Beck, S. M., et al., Operational overview of NASA GTE/CITE 1 airborne instrument intercomparisons: Carbon monoxide, nitric oxide, and hydroxyl instrumentation, *J. Geophys. Res.*, *92*, 1977–1985, 1987.

Bradshaw, J. D., and D. D. Davis, Sequential two-photon laser-induced fluorescence: A new method for detecting atmospheric trace levels of NO, *Opt. Lett.*, *7*, 224–226, 1982.

Bradshaw, J. D., M. O. Rodgers, S. T. Sandholm, S. Kesheng, and D. D. Davis, A two-photon laser-induced fluorescence field instrument for ground-based and airborne measurements of atmospheric NO, *J. Geophys. Res.*, *90*, 12,861–12,873, 1985.

Carroll, M. A., M. McFarland, B. A. Ridley, and D. L. Albritton, Ground-based nitric oxide measurements at Wallops Island, Virginia, *J. Geophys. Res.*, *90*, 12,853–12,860, 1985.

Crutzen, P. J., Gas phase nitrogen and methane chemistry in the atmosphere, in *Physics and Chemistry of Upper Atmospheres*, edited by B. M. McCormac, pp. 110–124, D. Reidel, Hingham, Mass., 1973.

Crutzen, P. J., The role of NO and NO_2 in the chemistry of the troposphere and stratosphere, *Annu. Rev. Earth Planet. Sci.*, *7*, 443–472, 1979.

DeMore, W. E., M. J. Molina, S. P. Sanders, D. M. Golden, R. F. Hampson, M. J. Kurylo, C. J. Howard, and A. R. Ravishankara, Chemical kinetics and photochemical data for use in stratospheric modeling evaluation number 8, *JPL Publ. 87-41*, Jet Propul. Lab., Pasadena, Calif., Sept. 15, 1987.

Ehhalt, D. H., and J. W. Drummond, The tropospheric cycle of NO_x, in *Chemistry of the Unpolluted and Polluted Troposphere*, edited by H. W. Georgii and W. Jaeschke, D. Reidel, Hingham, Mass., 1982.

Fahey, D. W., G. Hubler, D. D. Parrish, E. J. Williams, R. B. Norton, B. A. Ridley, H. B. Singh, S. C. Liu, and F. C. Fehsenfeld, Reactive nitrogen species in the troposphere: Measurement of NO, NO_2, HNO_3, particulate nitrate, peroxyacetyl nitrate (PAN), O_3, and total reactive odd nitrogen (NO_y) at Niwot Ridge, Colorado, *J. Geophys.Res.*, *91*, 9781–9793, 1986.

Finlayson-Pitts, B. J., and J. N. Pitts, *Atmospheric Chemistry: Fundamentals and Experimental Techniques*, John Wiley, New York, 1986.

Gregory, G. L., et al., An intercomparison of airborne nitrogen dioxide instruments, *J. Geophys. Res.*, this issue.

Hastie, D. R., G. I. Mackay, T. Iguchi, B. A. Ridley, and H. I. Schiff, Tunable diode laser systems for measuring trace gases in tropospheric air, *Environ. Sci. Technol.*, *17*, 352a–364a, 1983.

Hoell, J. M., et al., An intercomparison of carbon monoxide, nitric oxide, and hydroxyl measurement techniques: Overview results, *J. Geophys. Res.*, *89*, 11,819–11,825, 1984.

Hoell, J. M., G. L. Gregory, D. S. McDougal, A. L. Torres, D. D. Davis, J. D. Bradshaw, M. O. Rodgers, B. A. Ridley, and M. A. Carroll, Airborne intercomparison of nitric oxide measurement techniques, *J. Geophys. Res.*, *92*, 1995–2008, 1987.

Kley, D., and M. McFarland, Chemiluminescence detector for NO and NO_2, *Atmos. Technol.*, *12*, 63–69, 1980.

Logan, J. A., Nitrogen oxides in the troposphere: Global and regional budgets, *J. Geophys. Res.*, *88*, 10,785–10,805, 1983.

Logan, J. A., M. J. Prather, S. C. Wofsy, and M. B. McElroy, Tropospheric photochemistry: A global perspective, *J. Geophys. Res.*, *86*, 7210–7254, 1981.

McNeal, R. J., J. P. Mugler, R. C. Harriss, and J. M. Hoell, NASA Global Tropospheric Experiment, *Eos Trans. AGU*, *64*, 561–562, 1983.

Okabe, H., *Photochemistry of Small Molecules*, John Wiley, New York, 1978.

Ridley, B. A., and L. C. Howlett, An instrument for nitric oxide measurement in the stratosphere, *Rev. Sci. Instrum.*, *45*, 742–746, 1974.

Ridley, B. A., M. A. Carroll, A. L. Torres, E. P. Condon, G. W. Sachse, G. F. Hill, and G. L. Gregory, An intercomparison of results from ferrous sulfate and photolytic converter techniques for measurements of NO_x made during the NASA GTE CITE 1 aircraft program, *J. Geophys. Res.*, *93*, 15,803–15,811, 1988.

Rodgers, M. O., K. Asai, and D. D. Davis, Photofragmentation-laser induced fluorescence: A new method for detecting atmospheric trace gases, *Appl. Opt.*, *19*, 3597–3605, 1980.

Rodgers, M. O., J. D. Bradshaw, S. T. Sandholm, S. Kesheng, and D. D. Davis, A two-wavelength laser-induced fluorescence field instrument for ground-based and airborne measurements of atmospheric OH, *J. Geophys. Res.*, *90*, 12,819–12,834, 1985.

Schiff, H. I., D. R. Karecki, G. W. Harris, D. R. Hastie, and G. I. Mackay, A tunable diode laser system for aircraft measurements of trace gases, *J. Geophys. Res.*, this issue.

Singh, H. B., Reactive nitrogen in the troposphere: Chemistry and transport of NO_x and PAN, *Environ. Sci. Technol.*, *21*, 320–327, 1987.

J. D. Bradshaw, D. D. Davis, K. S. Dorris, M. O. Rodgers, and S. T. Sandblom, School of Earth and Atmospheric Sciences, Georgia Institute of Technology, Atlanta, GA 30332.

(Received January 17, 1989;
revised August 11, 1989;
accepted August 24, 1989.)